18.336 FINAL REPORT

LORENZO VAN MUÑOZ*

1. Introduction. In optics, the design of metamaterials is blurring the line between the traditions of geometric optics and diffractive optics by allowing the fine tuning of optical elements at a sub-wavelength scale. Often, the inverse design problem poses a huge computational challenge due to the demanding nature of full-wave simulations in 3D on large structures. As an alternative to full-3D simulations, metamaterials which are thin compared to the wavelengths of light incident upon them can be approximated by metasurfaces which have impedance data parametrized on a surface [5]. In this report I explore a fast and accurate boundary integral method that is only applicable to planar, 2D periodic metasurfaces with periodic boundary data and employs Fourier pseudospectral acceleration.

2. Problem formulation. The metasurface scattering problem considers a geometry of two half-spaces, Ω_1, Ω_2, separated by a plane Γ and tries to solve for the total electromagnetic fields given an incident planewave with wavenumber k. In the half spaces, the fields must satisfy Maxwell's curl equations:

$$-\mu \partial_t \boldsymbol{H} = \boldsymbol{\nabla} \times \boldsymbol{E} \tag{2.1}$$

$$\epsilon \partial_t \boldsymbol{E} = \boldsymbol{\nabla} \times \boldsymbol{H} \tag{2.2}$$

and on the plane, the fields must satisfy a local jump condition created by the metasurface's impedance parameters $Z_e = Y_e^{-1}$ and $Z_m = Y_m^{-1}$:

$$\hat{\boldsymbol{n}} \times (\boldsymbol{H}_2 - \boldsymbol{H}_1) = \frac{1}{2} Y_e (\boldsymbol{E}_2 + \boldsymbol{E}_1) \tag{2.3}$$

$$-\hat{\boldsymbol{n}} \times (\boldsymbol{E}_2 - \boldsymbol{E}_1) = \frac{1}{2} Y_m (\boldsymbol{H}_2 + \boldsymbol{H}_1). \tag{2.4}$$

In the equations above, $\hat{\boldsymbol{n}}$ is the normal vector to Γ and the subscripts on the fields denote the limiting value of that field in the specified half-space as it approaches the given point in Γ. These jump conditions on the tangential fields were first formulated in [5] as an effective medium description of thin scatterers such as flat antennae.

2.1. Boundary conditions. Beyond the jump conditions, the solution must also satisfy a radiation condition in the half-spaces that the fields must have uniformly-convergent Rayleigh-Bloch expansions as planewaves away from Γ [1].

Moreover, I restrict to the case that the metamaterial parameters, Y_e, Y_m, are periodic in two-dimensions. Namely, they satisfy $Y(x + nL_x, y + mL_y) = Y(x, y)$ for all $(x, y) \in \boldsymbol{R}^2$ given periods L_x, L_y. Lastly, the third dimension, z, is referred to as the scattering axis, and thus $\hat{\boldsymbol{n}} = \hat{\boldsymbol{z}}$.

2.2. Reduction to 2D. When simplifying the problem to 2D, I assume that the metasurface parameters are invariant in y so that all of their y derivatives vanish. In this setting, Maxwell's equations decouple into two independent equations for the transverse-electric (TE) and transverse-magnetic (TM) modes, which are governed by

*Department of Physics, Massachusetts Institute of Technology, 77 Massachusetts Avenue, Cambridge, MA 02139 (lxvm@mit.edu, http://web.mit.edu/lxvm/www/).

the solution to H_z and E_z. It can be derived that the PDEs for either mode reduce to the following Helmholtz problem in the half-planes [6]

$$\nabla^2 u + k^2 u = 0 \tag{2.5}$$

and the jump conditions on the curve

$$\partial_z(u_2 - u_1) = -ik\alpha(u_2 + u_1) \tag{2.6}$$

$$\partial_z(u_2 + u_1) = -ik\beta(u_2 - u_1). \tag{2.7}$$

Above we have introduced modified metasurface parameters α and β which are L-periodic and can be related back to the original parameters. The exact form depends on whether the problem is formulated for the TE or TM mode, and is not essential for the solution methods for the PDE.

2.3. Quasi-periodic Green's function. The exact solution of the problem can be obtained with a properly-formulated Green's function for the 2D PDE, $G(\boldsymbol{r}, \boldsymbol{r}')$, for a point source at $\boldsymbol{r} = (x, z)$ and a target point $\boldsymbol{r}' = (x', y')$. In the half planes, for $\boldsymbol{r} \in \Omega_1 \cup \Omega_2$, the Green's function must satisfy

$$\nabla^2_{\boldsymbol{r}} G(\boldsymbol{r}, \boldsymbol{r}') + k^2 G(\boldsymbol{r}, \boldsymbol{r}') = -\delta(\boldsymbol{r} - \boldsymbol{r}') \tag{2.8}$$

and on the metasurface, for $\boldsymbol{r} \in \Gamma$, the condition is

$$\partial_z(G_2(\boldsymbol{r}, \boldsymbol{r}') - G_1(\boldsymbol{r}, \boldsymbol{r}')) = -ik\alpha(G_2(\boldsymbol{r}, \boldsymbol{r}') + G_1(\boldsymbol{r}, \boldsymbol{r}')) \tag{2.9}$$

$$\partial_z(G_2(\boldsymbol{r}, \boldsymbol{r}') + G_1(\boldsymbol{r}, \boldsymbol{r}')) = -ik\beta(G_2(\boldsymbol{r}, \boldsymbol{r}') - G_1(\boldsymbol{r}, \boldsymbol{r}')). \tag{2.10}$$

In particular, the exact Green's function, G_{QP}, can be obtained from the free-space 2D Green's function, $G_0(\boldsymbol{r}, \boldsymbol{r}')$, given by

$$G_0(\boldsymbol{r}, \boldsymbol{r}') = \frac{i}{4} H_0^{(1)}(k|\boldsymbol{r} - \boldsymbol{r}'|) \tag{2.11}$$

where $H_0^{(1)}$ is a zero-th order Hankel function of the first kind. While G_0 satisfies the radiation condition, the periodicity can be achieved by summing phased copies on the periodic lattice of unit cells to obtain a quasi-periodic Green's function. This becomes

$$G_{QP}(\boldsymbol{r}, \boldsymbol{r}') = \frac{i}{4} \sum_{n=-\infty}^{\infty} e^{ik\cos(\theta)nL} H_0^{(1)}(k\sqrt{(x - x' + nL)^2 + (y - y')^2}) \tag{2.12}$$

where θ is the angle of incidence measured from the $\hat{\boldsymbol{x}}$ axis [1].

Numerical evaluation of the infinite sum in the quasi-periodic Green's function has received much attention and can be evaluated by methods such as Ewald summation and summation with a window function. Due to its simplicity, I implemented a windowed sum, which takes the following form:

$$G^A_{QP}(\boldsymbol{r}, \boldsymbol{r}') = \frac{i}{4} \sum_{n=-\infty}^{\infty} w_A(x - x' + nL) e^{ik\cos(\theta)nL} H_0^{(1)}(k\sqrt{(x - x' + nL)^2 + (y - y')^2}) \tag{2.13}$$

with the window function, w_A, defined by

(2.14)
$$w_A(x; x_0, x_1) = \begin{cases} 0 & \text{if } |x| \leq x_0 \\ \exp(2\exp(1/u)/(1-u)) & \text{if } x_0 < |x| < 1, u = (|x| - x_0)/(x_1 - x_0) \\ 1 & \text{if } |x| \geq x1 \end{cases}$$

It is known that integrals of periodic functions times the windowed Green's function converge superalgebraically with respect to the window size A [2].

Note that the quasi-periodic Green's function is ill-defined at points where $(k\cos(\theta)+nL)^2 = k^2$ for any integer n. This can be shown by applying the Poisson summation formula to G_{QP}. Such a point is called a Wood anomaly.

2.4. Integral formulation. We can solve the PDE as a boundary integral by using the Green's function and making the ansatz

$$u_i(\boldsymbol{r}) = \int_\Gamma G_{QP}(\boldsymbol{r}, \boldsymbol{r}')\sigma_i(\boldsymbol{r}')d\boldsymbol{r}'. \tag{2.15}$$

We equivalently write this as a single-layer operator, $u_i = S[\sigma_i]$. Then the jump conditions become [3]

$$u_2 + u_1 = S[\sigma_2 + \sigma_1] \tag{2.16}$$
$$u_2 - u_1 = S[\sigma_2 - \sigma_1] \tag{2.17}$$
$$\partial_z(u_2 + u_1) = -\frac{1}{2}(\sigma_2 - \sigma_1) \tag{2.18}$$
$$\partial_z(u_2 - u_1) = -\frac{1}{2}(\sigma_2 + \sigma_1) \tag{2.19}$$

and by introducing new variables $\xi_1 = \sigma_1 + \sigma_2, \xi_2 = \sigma_1 - \sigma_2$ we use the jump conditions to arrive at the following system of boundary integral equations

$$(-I/2 + ik\alpha(x)S)\xi_1 = -2ik\alpha(x)e^{ik\cos(\theta)x} \tag{2.20}$$
$$(-I/2 + ik\beta(x)S)\xi_2 = -2i\sqrt{k^2 - (k\cos(\theta))^2}e^{ik\cos(\theta)x}. \tag{2.21}$$

This integral formulation was derived by Carlos Pérez-Arancibia in an ongoing collaboration. Since these are integral equations of the second kind, they are favorable for iterative methods.

3. Spectrally accurate quadrature for closed boundaries. The Kress quadrature rule (originally due to Martensen and Kussmaul) was originally invented as a specialized quadrature for the single-layer operator with a logarithmic kernel, such as for G_{QP}. On closed curves, this method converges spectrally and faster than other quadratures, and is not FMM compatible since the quadrature rule globally modifies the kernel [4]. In this work, a notable difference is that we are performing an integral over an open curve, and as a result care must be taken to evaluate the kernel appropriately. In particular, a main difference I encountered in this work is that the quantity $x - x'$ can be evaluated directly for closed curves, but for open curves must be taken to be the minimum distances of $x - x'$ for all periodic images of x and x'.

3.1. Singularity separation. The Kress quadrature rule requires knowledge of the kernel, $K(x,x')$, and in particular a decomposition of the form $K(x,x') = K_1(x,x')\log\left(4\sin^2\left(\frac{x-x'}{2}\right)\right)+K_2(x,x')$, where K_1 and K_2 are analytic and 2π periodic [3]. In particular, for the 2D free space Green's function, G_0, such a decomposition is known

(3.1)
$$G_0(x,x') = \begin{cases} -\frac{1}{4\pi}J_0(k|x-x'|)\log\left(4\sin^2\left(\frac{x-x'}{2}\right)\right) + \frac{i}{4}H_0^{(1)}(k|x-x'|) & \text{if } x \neq x' \\ -\frac{1}{4\pi}J_0(k|x-x'|)\log\left(4\sin^2\left(\frac{x-x'}{2}\right)\right) + \left(\frac{i}{2} - \frac{\gamma}{2\pi} - \frac{1}{2\pi}\log\left(\frac{k}{2}\right)\right) & \text{if } x = x' \end{cases}$$

In the derivative above we assumed that Γ is a unit-speed parameterized curve of length 2π and used the Euler-Mascheroni constant γ.

To extend this decomposition to G_{QP}, note that the evaluation points can always be chosen around a single singularity of the quasi-periodic kernel, namely $x - x' = 0$, although there are singularities at all $x - x' = 0 \mod 2\pi$. The terms with $n \neq 0$ in the quasi-periodic sum can be evaluated regularly with the correction above applied only to the $n = 0$ term. However, a major limitation of the Kress quadrature on G_{QP} is that the remaining terms in the sum are not truly a periodic function unless $k\cos(\theta)L = 0 \mod 2\pi$, which corresponds to having the incident wave be exactly a Bloch mode providing periodic boundary data. Other projects may want to investigate if a singularity separation which does not distinguish $n = 0$ in the G_{QP} sum is available.

3.2. Nyström discretization. To discretize the single-layer operator we employ the following quadrature [4]

$$\int_0^{2\pi} K(x,x')\sigma(x')dx' \approx \sum_{j=1}^{2N} R_j^{(N)}(x)K_1(x,x_j)\sigma(x_j) + \frac{\pi}{N}\sum_{j=1}^{2N} K_2(x,x_j)\sigma(x_j) \tag{3.2}$$

where the quadrature nodes are chosen on an equispaced grid $x_j = j\pi/N$ and the weights $R_j^{(N)}(x)$ are given by

$$R_j^{(N)}(x) = -\frac{2\pi}{N}\left(\sum_{m=1}^{N-1}\frac{\cos(m(x_j-x))}{m} + \frac{\cos(N(x_j-x))}{2N}\right). \tag{3.3}$$

The target points can be chosen freely, but as will be explained below it is fastest to choose them to be on the same points as the quadrature grid.

4. Fast iterative solver. To convert the preceding quadrature into a fast method, it suffices to apply the second-kind Fredholm integral operator as a fast matrix-vector product, which can then be used in a general purpose iterative solver such as GMRES. This acceleration becomes increasingly important when dealing with small wavenumbers or rapidly-varying metasurface parameters that require finer discretizations of the boundary to resolve the solution. The main observation that will allow us to develop a fast method is that the discretization of S evaluated on equispaced nodes is a circulant matrix. This can be seen in (3.2) by noticing that when the source and target points are the same equispaced grid, the weights become a circulant matrix, and the distances, $|x_i - x_j|$, when interpreted in a periodic fashion are also circulant.

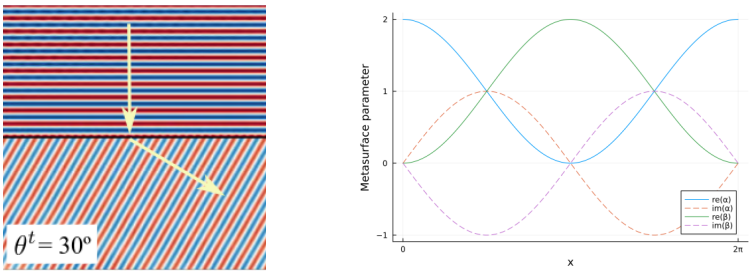

FIG. 1. *Representative geometry of the 2D metasurface scattering problem and parameters of a metasurface which deflects an incident planewave to an outgoing planewave with a new wavevector. This metasurface only accomplishes its goal for a single wavenumber and a single set of incident and outgoing wavevectors. Leftmost figure was taken from [6]. Generally the periodic metasurface, which acts as a diffraction grating, can only couple Bloch wavevectors on either side of the surface.*

4.1. Fourier pseudospectral matrix-vector product. When S is a circulant matrix, denote one of its columns by s and observe that the product $S\xi$ is equal to the circular convolution $s \star \xi$. In Fourier space, this operation is equivalent to point-wise multiplication, i.e. $\widehat{s \star \xi} = \hat{s}\hat{\xi}$. Let $\mathcal{F}$ denote the discrete Fourier transform matrix. The fast matrix-vector product is given by

$$(-I/2 + ik\alpha(x)S) = \mathcal{F}^{-1}(-I/2 + ik\mathcal{F}\alpha(x)\mathcal{F}^{-1}\hat{s})\mathcal{F}. \tag{4.1}$$

Compared to a direct solver with $\mathcal{O}(N^3)$ complexity, this matrix-vector product is a $\mathcal{O}(N\log(N))$ operation whose complexity stays the same if GMRES converges in a fixed number of operations, giving a fast method for the solution of the auxiliary densities ξ_1, ξ_2 and thus the surface densities σ_1, σ_2.

5. Results. In this section I present results for a single metasurface and compare the convergence and timings of both fast and direct solvers.

5.1. Problem parameters. The metasurface illustrated in Fig. 1 was shown in [6] to deflect an incident wave of wavenumber k at angle θ_i to another wave at angle θ_t. The analytic form of the metasurface parameters is

$$\alpha(x) = -\sin(\theta_i)\left(1 + e^{ikd}\right) \tag{5.1}$$

$$\beta(x) = -\sin(\theta_i)\left(1 - e^{ikd}\right) \tag{5.2}$$

where $d = \cos(\theta_t) - \cos(\theta_i)$ and the metasurface period is $L = 2\pi/k|d|$. In the calculations that follow, I take $k = 10, \theta_i = -\pi/2, \theta_t = -\pi/6$. This corresponds to deflecting a normally incident wave by 60 degrees. The calculation could be more difficult with more quickly varying metasurface parameters or with a more oblique θ_i that is still a Bloch mode for the given wavenumber, but this mild parameter choice is good for validation.

In Fig. 2 are solutions for the surface densities and fields for the specified problem. They display the same periodicity that exists in metasurface and boundary data, although they are more rapidly varying.

5.2. Convergence tests. Fig. 3 presents self-convergence results for the direct solver, and the results are identical for the fast solver. Unlike Kress quadrature on a closed surface, the rate of convergence is only analytic in this problem with an open surface. Still, the solution converges rapidly with 4th order convergence, giving a

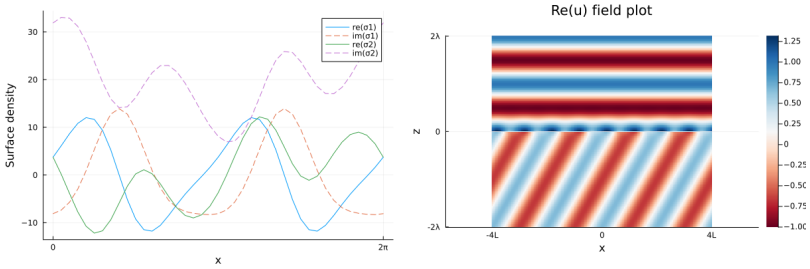

FIG. 2. *Solutions of the deflecting metasurface scattering problem with parameters* $k = 10, \theta_i = -\pi/2, \theta_t = -\pi/6$. *The line plot displays the real and imaginary parts of the surface current densitites above and below the metasurface as obtained by the solver. The heatmap displays the real part of the fields, which clearly depict the normally-incident planewave from above the sheet being deflected to an obliquely-outgoing planewave.*

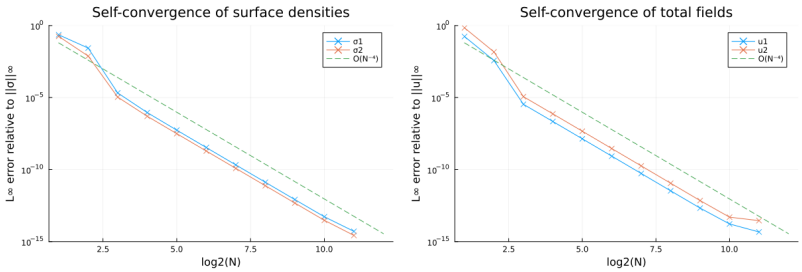

FIG. 3. *The spectrally-accurate Kress quadrature rule used in this report appears to only yield algebraic convergence in the solution of the surface current densities and the fields, which were evaluated at a distance of one wavelength away from the metasurface. In fact, this is due to treatment of the quasi-periodic Green's function, which is windowed and thus not truly periodic, and moreover, is only corrected with the Kress quadrature rule at one of the singularities, therefore breaking the periodicity. Nonetheless, the rate of algebraic convergence that can be seen in the surface density plots is* $\mathcal{O}(N^{-4})$ *and is sufficiently rapid to obtain 10 digits of accuracy when requesting* $N = 128$.

practical solver that converges in a modest number of grid points. Possibilities of why the convergence is not spectral include bugs as well as an imperfect singularity cancellation in the Kress quadrature for G_{QP}, which may be sensitive to the windowed sum. Taking more difficult metasurface or scattering parameters may also slow the rate of convergence.

5.3. Method scaling. Fig. 4 present the scaling of the direct solver, $\mathcal{O}(N^3)$ versus the fast solver, $\mathcal{O}(N \log(N))$. The implementations are both in very good agreement with the asymptotic scalings for $N > 100$.

In summary, Table 1 presents timings and errors for the Kress quadrature with direct and fast methods. The crossover of the fast method over the direct solver is apparent at $N = 32$, where the relative error is already at the 8th significant digit. Clearly while high-order methods converge quickly enough to not need many grid points, the fast method has a small enough constant to make it competitive in most cases.

5.4. Code availability. The implementation of the direct and fast solvers is available at the following repository https://github.com/lxvm/MetaBIE.git. Generating the data, figures, and report is as simple as running a shell script and takes about ten minutes.

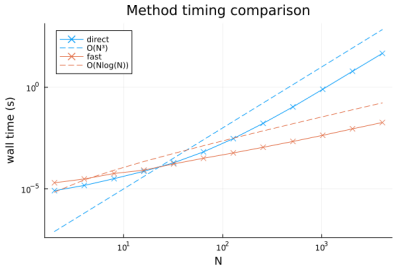

FIG. 4. *Wall clock time versus N comparing the direct solver and fast solver for calculating the surface densities of the deflecting metasurface with parameters $k = 10, \theta_i = -\pi/2, \theta_t = -\pi/6$. All calculations were performed on a single core of an Intel i5-12500 processor, and they include the time to evaluate the boundary data, construct the single-layer operator, and solve the linear system. The only cached data used were the Kress quadrature weights and FFTW plans.*

N	Direct timing (s)	Fast timing (s)	Relative error
2^5	0.00019	0.00017	5.4e–08
2^7	0.00297	0.00060	2.1e–10
2^9	0.11071	0.00222	8.2e–13
2^{11}	6.33158	0.00944	5.1e–15

TABLE 1

Representative timings and relative errors taken from the preceding plots comparing the speed of the two solvers and the relative error in the surface density of their solution. The relative error displayed is the maximum relative error of either the surface density above or below the sheet.

6. Discussion. The most interesting result of this work has been to discover that the convergence of the Kress quadrature in this case with an open boundary is only algebraic with 4th order convergence. Although I can't rule out the possibility of a bug, a more careful analysis of the singularity separation for G_{QP} may be able to reveal the origin of the algebraic rate. Further investigation also is necessary to determine whether the boundary integral formulation of the full 3D problem still reduces to either a circulant or block-circulant representation that is compatible with the Fourier pseudospectral method employed in this report. Additionally, it would be worthwhile to pursue other quadrature rules which can recover spectral convergence in the presence of both periodic and quasi-periodic boundary data while also being accelerated by either the method in this report or an FMM, which would have to use a potential expansion tailored to the quasi-periodic Green's function. In my previous research, I have developed a Fourier spectral method solver for the 3D problem, which also obtains $\mathcal{O}(N \log(N))$ complexity if solved using iterative method, and believe that it should be the easiest path to a fast 3D solver if I can resolve some numerical conditioning issues that arise in the method.

REFERENCES

[1] A. BARNETT AND L. GREENGARD, *A new integral representation for quasi-periodic scattering problems in two dimensions*, BIT Numerical Mathematics, 51 (2011), pp. 67–90, https://doi.org/10.1007/s10543-010-0297-x.

[2] O. P. BRUNO, M. LYON, C. PÉREZ-ARANCIBIA, AND C. TURC, *Windowed Green Function Method for Layered-Media Scattering*, SIAM Journal on Applied Mathematics, 76 (2016), pp. 1871–1898, https://doi.org/10.1137/15M1033782.

[3] D. COLTON AND R. KRESS, *Inverse Acoustic and Electromagnetic Scattering Theory*, vol. 93 of

Applied Mathematical Sciences, Springer, New York, NY, 2013, https://doi.org/10.1007/978-1-4614-4942-3.

[4] S. Hao, A. H. Barnett, P. G. Martinsson, and P. Young, *High-order accurate Nystrom discretization of integral equations with weakly singular kernels on smooth curves in the plane*, Nov. 2012, https://doi.org/10.48550/arXiv.1112.6262, https://arxiv.org/abs/1112.6262.

[5] E. Kuester, M. Mohamed, M. Piket-May, and C. Holloway, *Averaged transition conditions for electromagnetic fields at a metafilm*, IEEE Transactions on Antennas and Propagation, 51 (2003), pp. 2641–2651, https://doi.org/10.1109/TAP.2003.817560.

[6] C. Pérez-Arancibia, R. Pestourie, and S. G. Johnson, *Sideways adiabaticity: Beyond ray optics for slowly varying metasurfaces*, Optics Express, 26 (2018), pp. 30202–30230, https://doi.org/10.1364/OE.26.030202.